

Antoni Sawicki

Mathematical Differential and Integral Models in the Macromodelling of Electric Arc Using Voltage and Current Controlled Sources

Part 1. Variants of Electric Arc Macromodels Obtained from Various Forms of Differential or Integral Equations

Abstract: The article presents justification for creating mathematical models of electric arc in differential and integral forms as well as discusses simple variants of classic mathematical arc models with indefinite or unreduced ignition voltage and variants of modified mathematical arc models with specified or reduced ignition voltage. In addition, the article discusses hybrid mathematical models of electric arc in differential and integral forms. and presents the above-named variants in the non-rationalised form (with function dependencies determined by arc current) and in the rationalised form (with functional dependencies determined by column conductance). The effectiveness of various macromodels was verified by simulating processes in circuits with electric arc.

Keywords: electric arc, Mayr model, Cassie model, hybrid model

DOI: [10.17729/ebis.2019.6/7](https://doi.org/10.17729/ebis.2019.6/7)

Introduction

Because of the heterogeneous structure of electric arc it is convenient to break down the area of discharge into quasi-homogenous layers including the column with equilibrium plasma and very thin near-electrode layers containing non-equilibrium plasma. Near-electrode voltage drops depend on the material of electrodes and the efficiency of their cooling as well as on the temperature, pressure and physicochemical properties of plasma-forming gases. It is usually assumed that values of voltage are constant and independent of the value of current (approximately 12-35 V). Depending on the value of arc voltage it is possible to

take into consideration or ignore near-electrode voltage drops. If arc is short (e.g. free welding arc), plasma columns are characterised by low values of voltage. In such cases, it is necessary to take into consideration near-electrode voltage drops. In cases of high values of voltage (long arc), the aforesaid drops can be ignored. The latter approach can simplify the creation of macromodels of arc in simulation programmes and during the design and construction of welding arc simulators [1-3]. For this reason, experimental tests of arc and the determination of arc parameters are subordinate to experiments revealing electric properties of plasma layers [4].

Antoni Sawicki, PhD (DSc) Habilitated Eng.

SEP – Stowarzyszenie Elektryków Polskich (FSNT-NOT) /Association of Polish Electrical Engineers/, Częstochowa

When creating macromodels of electric arc it is necessary to model the static or dynamic properties of a physical object using non-linear resistance. The simplest synthesis of such a resistor usually comes down to the selection of an appropriate virtual source of energy, where voltage is directed oppositely to the flow of current or current is directed oppositely to present voltage. Under such conditions, the element plays the role of a proper receiver, dissipating energy as a regular resistor. As arc is a strongly non-linear element, related sources must be controlled using voltage or current formed by components of mathematical models of arc. The selection of such components and mathematical operations performed by them depend on an adopted (differential or integral) form of the aforesaid model. Some of them may facilitate, whereas others may impede the formation of a macromodel as well as may affect the accuracy and stability of numerical calculations. For this reason, the knowledge of variants of mathematical models of arc is of significance when attempting to obtain the required accuracy of the approximation of experimental data as well as the speed and stability of numerical calculations.

Classical and modified differential and integral models of electric arc

The creation of a non-linear load modelling electric properties of arc requires the solving of the functional dependence between voltage and current $f(u, i) = 0$, resulting from the power balance equation [1]. The above-named solution can be obtained using one of the two methods presented below:

1. voltage u on the arc column is obtained by means of a converter converting voltage u into conductance g , and, subsequently, into voltage u , which, is performed by means of an appropriate voltage follower ($u \rightarrow g(u, i) \rightarrow u(g)$);
2. current i w the arc column is obtained using a converter converting voltage u into conductance g , and, subsequently, into current ($u \rightarrow g(u) \rightarrow i(g)$);

The first method enabling the development of macromodels in computer software programmes and arc simulators [1] is easier as it makes it possible to separately imitate voltage on the plasma column and in near-electrode areas. As a result, the aforesaid method can be used to simulate processes in circuits with short (e.g. welding) arc. The second method of macromodel development is more complicated. It is not possible to easily isolate components of resultant arc voltage. For this reason, after ignoring the aforesaid components, the method can be used to create approximate macromodels of long (high-voltage) arc [5-7]. The simplified and, at the same time, approximate method of simulating dynamic properties of arc involves treating near-electrode voltage drops as component of voltage dependent on the length of column $l \propto U_C$.

Table 1. Classical differential and integral mathematical models of arc with unspecified or unreduced ignition voltage (M1d, M1i –Mayr type models; M3d, M3i - Mayr-Schwartz type models; C1d, C1i - Cassie type models; C3d, C3i - Cassie-Schwartz type models)

Designation	Differential form of the model	Designation	Integral form of the model
M1d	$\theta_M \frac{dg}{dt} + g = \frac{i^2}{P_M}$	M1i	$g = g_0 \exp\left(\frac{1}{\theta_M} \int \left(\frac{ui}{P_M} - 1\right) dt\right)$
M3d	$\theta_{Ms}(g) \frac{dg}{dt} + g = \frac{i^2}{p_{Ms} g^\alpha}$	M3i	$g = g_0 \exp\left(\int \frac{1}{\theta_{Ms}(g)} \left(\frac{ui}{p_{Ms} g^\alpha} - 1\right) dt\right)$
C1d	$\theta_C \frac{dg^2}{dt} + g^2 = \frac{i^2}{U_C^2}$	C1i	$g = g_0 \exp\left(\frac{1}{2\theta_C} \int \left(\frac{u^2}{U_C^2} - 1\right) dt\right)$
C3d	$\theta_{Cs}(g) \frac{dg^2}{dt} + g^2 = \frac{i^2}{u_{Cs}^2 g^{2\beta}}$	C3i	$g = g_0 \exp\left(\int \frac{1}{2\theta_{Cs}(g)} \left(\frac{u^2}{u_{Cs}^2 g^{2\beta}} - 1\right) dt\right)$

Table 1 contains classical mathematical arc models with unspecified or unreduced ignition voltage [8]. Each of the models is presented in two, i.e. differential and integral, variants. The development of macromodels involving the use of the differential form requires knowing excitation current i . In addition, to calculate the value of conductance g it is necessary to measure the value of arc voltage u . The development of macromodels involving the use of the integral form requires knowing voltage u . In addition, to calculate the value of conductance g it is necessary to measure the value of arc current i . The designations of differential models adopted in the Table are the same as those used in publication [8].

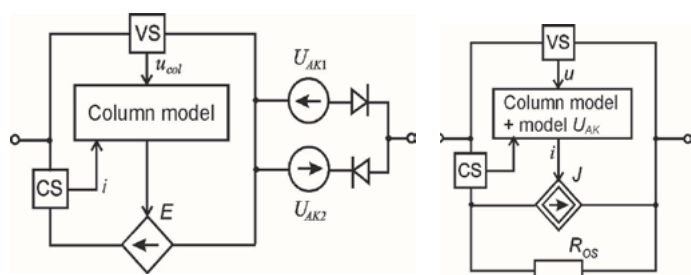


Fig. 1. Schematic diagrams of welding arc simulators:

- a) utilising the controlled source of voltage E ;
- b) utilising the controlled source of current J

(VS – voltage sensor; CS – current sensor; R_{OS} – decoupling resistor; U_{AK1} , U_{AK2} – sources modelling sums of near-electrode voltage drops; i , u_{col} – arc column current and voltage, u – voltage between electrodes)

Formulas presented in Table 1 contain the following designations: q_M – time constant of the Mayr model, $\theta_M(g)$ – damping function of the Mayr-Schwartz model, θ_C – time constant of the Cassie model, $\theta_{Cs}(g)$ – damping function of the Cassie-Schwartz model, PM – constant dissipated power of the Mayr model, $p_{Ms}(g)$ – coefficient of the dissipated power of the Mayr-Schwartz model, U_C – constant voltage of the Cassie model, u_{Cs} – voltage coefficient of the Cassie-Schwartz model, g_0 – integration constant.

In the differential mathematical Schwartz models, the variation of the time constant usually adopts the form of the power function, which is not the most favourable approximation in comparison with the application of the exponential function [9-11]. Sometimes, instead of the power function, used for the approximation of dissipated power $P(g)$, polynomial functions are used [12, 13].

The analysis of Table 1 leads to the development of various schematic diagrams related to the design of two variants of electric arc macromodels (Fig. 1). In the first case, utilising the controlled source of voltage, it is necessary to measure arc current and, frequently, also arc voltage. Processes occurring in the arc column are modelled using the differential model.

Table 2. Modified differential and integral mathematical models of arc with defined or reduced ignition voltage (M2d, M2i –Mayr type models; M4d, M4i – Mayr-Schwartz type models; C2d, C2i – Cassie type models; C4d, C4i – Cassie-Schwartz type models)

Designation	Differential form of the model	Designation	Integral form of the model
M2d	$\theta_M \frac{dg}{dt} + g = \frac{i^2 + I_w^2}{P_M} = \frac{i^2}{P_M} + G_{w0}$	M2i	$g = g_0 \exp\left(\frac{1}{\theta_M} \int \left(\frac{ui}{P_M} - 1 + \frac{G_{w0}}{g}\right) dt\right)$
M4d	$\theta_{Ms}(g) \frac{dg}{dt} + g = \frac{i^2 + I_w^2}{p_{Ms}g^\alpha}$	M4i	$g = g_0 \exp\left(\int \frac{1}{\theta_{Ms}(g)} \left(\frac{u^2g^2 + I_w^2}{p_{Ms}g^{\alpha+1}} - 1\right) dt\right)$
C2d	$\theta_C \frac{dg^2}{dt} + g^2 = \frac{(i + I_w)^2}{U_C^2} = \left(\frac{ i }{U_C} + G_{w0}\right)^2$	C2i	$g = g_0 \exp\left(\frac{1}{2\theta_C} \int \left(\left(\frac{ u }{U_C} + \frac{G_{w0}}{g}\right)^2 - 1\right) dt\right)$
C4d	$\theta_{Cs}(g) \frac{dg^2}{dt} + g^2 = \frac{(i + I_w)^2}{u_{Cs}^2 g^{2\beta}}$	C4i	$g = g_0 \exp\left(\int \frac{1}{2\theta_{Cs}(g)} \left(\frac{(u g + I_w)^2}{u_{Cs}^2 g^{2\beta+2}} - 1\right) dt\right)$

In turn, in the second case, utilising the controlled source of current, it is necessary to measure arc voltage and, frequently, also current flowing through the load [14]. To prevent the deterioration of structures of power supply systems and simulation instability, decoupling resistor R_{os} of a relatively high value is connected in parallel to the source of current. In such a case, processes occurring in the arc column are modelled using the integral model.

In certain cases related to the development and use of electric arc macromodels it is convenient to apply modified models with defined or reduced ignition voltage [8, 15, 16]. It can be easily done by modifying the models presented in Table 1 and obtaining the models presented in Table 2.

The formulas presented in Table 2 are provided with an additional designation, i.e. I_w – current corresponding to ignition voltage [11]. The aforesaid current also corresponds to residual conductance $G_{w_0} = I_w/U_C$ [8].

Differential and integral hybrid models of electric arc

Simple mathematical models (Table 1) are usually used to approximate dynamic characteristics of arc within narrow ranges of changes in excitation current. The extension of the above-named ranges necessitated the development of hybrid models, which, by means of tapering function $e(i)$, combine simple models into a parallel-structured system [10]. Similar to simple mathematical models of arc, also hybrid models can be used to create macromodels using voltage or current sources. For this reason, it is justified to present them in the differential and integral form.

The hybrid model of arc, combining the modified Mayr and Cassie sub-models can be presented in the following non-rationalised differential form [11]

$$g = \varepsilon'(i) \frac{i^2 + I_w^2}{P_M} + [1 - \varepsilon'(i)] \frac{i^2}{gU_C^2} - \theta'(i) \frac{dg}{dt} \quad (1).$$

After the introduction of the notion of residual conductance $G_w = I_w^2/P_M$ it is possible to obtain the following dependence

$$g = \varepsilon'(i) \left(\frac{i^2}{P_M} + G_w \right) + [1 - \varepsilon'(i)] \frac{i^2}{gU_C^2} - \theta'(i) \frac{dg}{dt} \quad (2),$$

where $\theta'(i)$ - damping function approximating experimental data within a wide range of changes in current [10]. Depending on the type of electric arc and the required accuracy of approximation, tapering function ε' can have a different analytical form [17].

In terms of the non-rationalised hybrid model, composed of the Mayr sub-model ($U = P_w/I, G_w = 0$) and of the Cassie sub-model ($U = U_C, P_{ri}(i) = 0$), it is possible to determine coordinate I_0 of the point of intersection of static characteristics

$$I_0 = \frac{P_M}{U_C} \quad (3).$$

In practical calculations, the value of current I_0 is relatively low. If appropriate components of the hybrid model are modified and have non-zero values, the usable condition of the intersection of static characteristics of the sub-models can be expressed as follows:

$$I_0 \cong \frac{P_M + \sqrt{P_M^2 - 4U_C^2 I_w^2}}{2U_C} = \frac{P_M + \sqrt{P_M^2 - 4P_M U_C^2 G_w}}{2U_C} \quad (4).$$

The integral form of non-rationalised hybrid model (1) can be expressed as follows

$$g = g_0 \exp \left\{ \int \frac{1}{\theta'(i)} \left[\varepsilon'(i) \left(\frac{ui}{P_M} + \frac{I_w^2}{gP_M} \right) + [1 - \varepsilon'(i)] \frac{ui}{gU_C^2} - 1 \right] dt \right\} \quad (5),$$

or, using model (2), as follows

$$g = g_0 \exp \left\{ \int \frac{1}{\theta'(i)} \left[\varepsilon'(i) \left(\frac{ui}{P_M} + \frac{G_w}{g} \right) + [1 - \varepsilon'(i)] \frac{ui}{gU_C^2} - 1 \right] dt \right\} \quad (6).$$

Based on experimental tests it is possible to determine the actual damping function [9].

If the function is non-linear, it is convenient to approximate it using dependence [10]

$$\theta'(i) = \theta_{i0} + \theta_{i1} \exp(-\alpha_i |i|) \approx \begin{cases} \theta_{i1}, & \text{if } |i| \text{ is low} \\ \theta_{i0}, & \text{if } |i| \text{ is large} \end{cases} \quad (7),$$

where $\alpha_i > 0$, $\theta_{i1} \gg \theta_{i0} > 0$ s – constant approximation coefficients.

Publication [10] also contain an assumption concerning a tapering function having the Gaussian form

$$\varepsilon'(i) = \exp\left(-\frac{i^2}{I_0^2}\right) \quad (8).$$

The physically justified rationalisation of hybrid models of arc (1) and (2) provides for the dependence of damping function $\theta''(g)$ and tapering function $\varepsilon''(g)$ on column conductance g . This leads to differential equations of a slightly different form and correct within wide ranges of changes in conductance g . The above-named equations can be expressed as follows [11]

$$g = \varepsilon''(g) \frac{i^2 + I_w^2}{P_M} + [1 - \varepsilon''(g)] \frac{i^2}{gU_c^2} - \theta''(g) \frac{dg}{dt} \quad (9)$$

or

$$g = \varepsilon''(g) \cdot \left(\frac{i^2}{P_M} + G_w \right) + [1 - \varepsilon''(g)] \frac{i^2}{gU_c^2} - \theta''(g) \frac{dg}{dt} \quad (10)$$

In the simplified case of the rationalised hybrid model, composed of the Mayr sub-model ($U = P_M/I$, $G_w = 0$) and the Cassie sub-model ($U = U_c$, $P_{rg} = 0$), it is possible to determine coordinate G_0 of the point of intersection of static characteristics of the sub-models

$$G_0 = \frac{P_M}{U_c^2} \quad (11).$$

In practical calculations, the value of conductance G_0 is relatively low. If appropriate

components of the hybrid model are modified and have non-zero values, the usable condition of the intersection of static characteristics can be expressed as follows:

$$G_0 \cong \frac{P_M + \sqrt{P_M^2 - 4U_c^2 I_w^2}}{2U_c^2} = \frac{P_M + \sqrt{P_M^2 - 4P_M U_c^2 G_w}}{2U_c^2} \quad (12).$$

The point of the intersection of the static characteristics of the models having non-linear functions dependent on current and the models having non-linear functions dependent on conductance is characterised by the following dependence

$$G_0 = \frac{I_0}{U_c} \quad (13).$$

The integral form of the hybrid model rationalised as presented above (9) is the following

$$g = g_0 \exp \left\{ \int \frac{1}{\theta''(g)} \left[\varepsilon''(g) \left(\frac{ui}{P_M} + \frac{I_w^2}{gP_M} \right) + [1 - \varepsilon''(g)] \frac{ui}{gU_c^2} - 1 \right] dt \right\} \quad (14),$$

or, based on (10), can be expressed as

$$g = g_0 \exp \left\{ \int \frac{1}{\theta''(g)} \left[\varepsilon''(g) \left(\frac{ui}{P_M} + \frac{G_w}{g} \right) + [1 - \varepsilon''(g)] \frac{ui}{gU_c^2} - 1 \right] dt \right\} \quad (15).$$

In the rationalised models, the damping function can adopt the form of a non-linear function dependent on conductance [11]

$$\theta''(g) = \theta_{g0} + \theta_{g1} \exp(-\alpha_g g) \approx \begin{cases} \theta_{g1}, & \text{if } g \text{ is low} \\ \theta_{g0}, & \text{if } g \text{ is large} \end{cases} \quad (16),$$

where $\alpha_g > 0$, $\theta_{g1} \gg \theta_{g0} > 0$ s – constant approximation coefficients. The adopted tapering function has the following form

$$\varepsilon''(g) = \exp\left(-\frac{g}{G_0}\right) \quad (17).$$

Results of simulation tests related to differential and integral models of arc using voltage and current sources in macromodels of arc

The above-presented theoretical analysis was used to expand the library of electric arc macromodels. Each case involved the performance of numerous tests using a set of parameters similar to experimental data and providing the stability of numerical calculations. One of important indicators of application efficiency of proposed models (and macromodels) was computing time. However, usually models of arc constitute just one of many elements of a complex electronic (welding equipment) or electrotechnical (electric joining equipment) systems. Because of very low values of the damping function, arc models are responsible for the tautness of differential equations, making users of simulation programmes apply special procedures of numerical calculations.

Macromodels of electric arc developed using differential models and controlled sources of voltage have been investigated by the author and discussed in many publications [2-4, 8, 11, 16, 17]. This study is concerned with results of simulations of integral models involved with the use of controlled sources of current. After selecting constant factors, each case involved the comparison of effects resulting from the use of differential and integral models. As expected, no significant differences between results obtained using the aforesaid methods. The tests involved typical simple electric circuits with active current excitation characterised by the sinusoidal wave and a frequency 50 Hz. In the Mayr model variants, current having an amplitude of 50 A was used. In turn, various variants of the Cassie model or the hybrid models involved the use of current having an amplitude of 150 A. At the above-named stage of the tests, near-electrode voltage drops were not implemented in the models.

The article presents selected results of simulation tests. Figure 2a presents the dynamic characteristic of arc described using the typical Mayr model in the integral form (M1i).

In turn, Figure 2b presents the characteristic of the modified Mayr-Schwartz model in the integral form (M4i), where, in addition to the variation of dissipation power, the variation of the time constant was used. The damping function had the typical power form

$$\theta_{Ms}(g) = f_{\theta} \cdot g^{\gamma} \quad (18),$$

where f_{θ} - constant factor, $sS^{-\gamma}$. Parameter I_w determines the voltage of discharge ignition [8]. The parameter is related to the value of residual conductance G_w when current passes through the zero value. The shapes of both characteristics are very similar, although the Schwartz modification enables the more precise approximation of experimental data within a wider range of current changes.

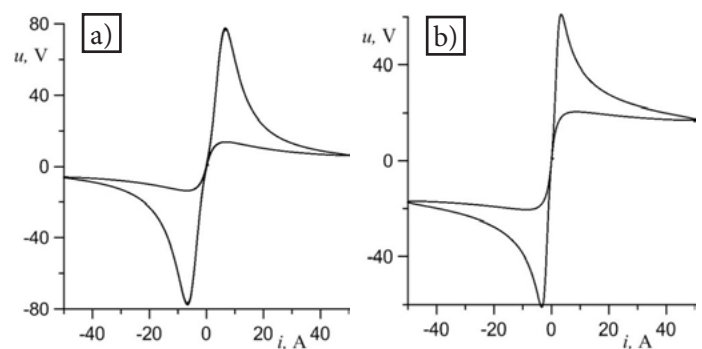


Fig. 2. Dynamic current-voltage characteristics obtained using: a) model M1i ($P_M = 300$ W, $\theta_M = 3 \cdot 10^{-4}$ s), b) model M4i ($P_{Ms} = 500$ A²/S^{a+1}, $a = 0.5$, $I_w = 0.5$ A, $f_{\theta} = 3 \cdot 10^{-4}$ sS^{-γ}, $\gamma = 0.2$)

Figure 3a presents the current voltage characteristic of arc described by the typical Cassie model C1i in the integral form. Figure 3b presents a curve being the result of simulation in the circuit with the modified integral Cassie-Schwartz model (C4i). In the above-named case, the damping function also had form (18).

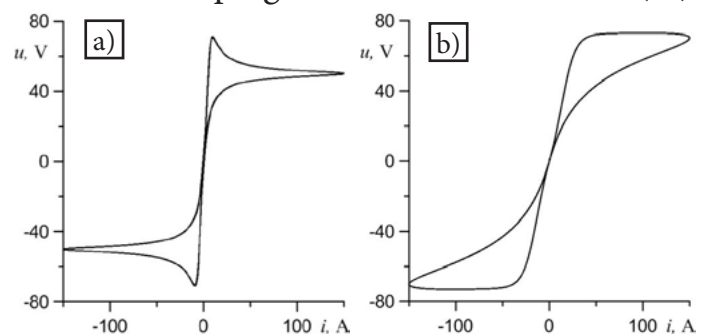


Fig. 3. Dynamic current-voltage characteristics obtained using: a) model C1i ($U_C = 50$ V, $\theta_C = 1 \cdot 10^{-4}$ s), b) model C4i ($u_{Cs} = 60$ V/S^{2β}, $\beta = 0.2$, $I_w = 1$ A, $f_{\theta} = 1 \cdot 10^{-3}$ sS^{-γ}, $g = 0.1$)

A relatively accurate approximation of experimental data can be obtained using hybrid models. Figure 4a presents the results of simulated processes in the circuit with the integral model described by equation (5), where the non-rationalised current-related functional dependences were used. A similar diagram of the dynamic characteristic of arc was obtained in relation to the rationalised integral model (14) – see Figure 4b.

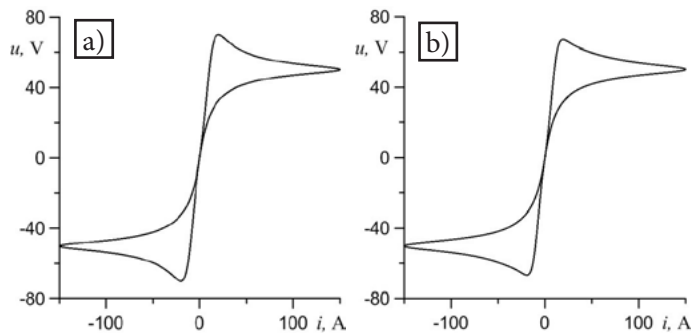


Fig. 4. Dynamic current-voltage characteristics obtained using: a) model (5) ($P_M=300\text{W}$, $U_C=50\text{V}$, $\theta_{i0} = 1 \cdot 10^{-5} \text{ s}$, $\theta_{i1} = 2 \cdot 10^{-4} \text{ s}$, $\alpha_i = 0.001$, $I_W = 0.5 \text{ A}$); b) model (14) ($P_M=300\text{W}$, $U_C=50\text{V}$, $\theta_{g0} = 1 \cdot 10^{-5} \text{ s}$, $\theta_{g1} = 2 \cdot 10^{-4} \text{ s}$, $\alpha_g = 0.001$, $I_W = 0.5 \text{ A}$)

Conclusions

1. The above-presented relatively large set of the differential and integral mathematical models of arc can find extensive applications in computer-aided simulations of dynamic states of electrotechnical equipment featuring arc or plasma-based heating.
2. The mathematical models of arc can be used in the construction and operation of welding arc simulators.
3. Preferences as to the selection of a given form of a mathematical model may result from required computational accuracy and the stability of the operation of a simulation programme.
4. Selected integral mathematical models are applied when simulating systems characterised by particularly unstable electric discharge (e.g. gliding arc plasmatron).

References:

[1] Верецаго Е.Н., Костюченко В. И.: Имитационная модель электрической

дуги, Электротехника, 6, 2014, pp. 36-42.

- [2] Sawicki A.: Imitatory łuków w diagnostyce źródeł spawalniczych. XLIX Międzyuczelniana Konferencja Metrologów MKM 2017, Koszęcin 4-6.09.2017, Zeszyty Naukowe Wydziału Elektrotechniki i Automatyki Politechniki Gdańskiej no. 54, pp. 195-198.
- [3] Sawicki A.: Diagnostyka imitatorów łuku z określonym lub zredukowanym napięciem zapłonu. Konferencja MKM 2019, Opole-Moszna 23-25.09.2019. Zeszyty Naukowe Wydziału Elektrotechniki i Automatyki Politechniki Gdańskiej, no. 66, pp. 79-84. (doi: 10.32016/1.66.17)
- [4] Sawicki A., Haltof M.: Wybrane metody eksperymentalnego wyznaczania przyelektrodowych spadków napięcia łuków elektrycznych. Cz. 1. Metody bezpośrednie wyznaczania przyelektrodowych spadków napięcia. Biuletyn Instytutu Spawalnictwa 2015, no. 6, pp. 61-69. (Selected Methods Used in Experimental Determination of Near-Electrode Voltage Drops of Electric Arcs. Part 1: Direct Methods Used in Determination of Near-Electrode Voltage Drops, p. 52-62. Internet). <http://bulletin.is.gliwice.pl/article/selected-methods-used-experimental-determination-near-electrode-voltage-drops-electric-arcs-part-1>
- [5] Jaroszyński L., Stryczewska H.D.: Computer simulation of the electric discharge in gliding arc plasma reactor. Conference: 3rd International Conference: Electromagnetic devices and processes in environment protection ELMECO-3, June 2000
- [6] Jaroszyński L., Stryczewska H.D.: The numerical model of the gliding arc discharge. II International Symposium: New Electrical and Electronic Technologies and Their Industrial Implementation NEET'2001, February 2001.
- [7] Jaroszyński L., Stryczewska H.D.: Analiza numeryczna urządzeń wyładowczych

- na przykładzie reaktora plazmowego ze ślizgającym się wyładowaniem łukowym. Prace Naukowe Instytutu Podstaw Elektrotechniki i Elektrotechnologii Politechniki Wrocławskiej. Konferencje Vol. 37, no. 12, 2000, pp. 331-335.
- [8] Sawicki A.: Klasyczne i zmodyfikowane modele matematyczne łuku elektrycznego. Biuletyn Instytutu Spawalnictwa 2019, no. 4, pp. 73-76.
<http://bulletin.is.gliwice.pl/article/non-linear-and-parametric-mathematic-models-electric-arcs>
- [9] Kalasek V.: Measurements of time constants on cascade d.c. arc in nitrogen. TH-Report 71-E18, Eindhoven 1971, p. 1-30.
- [10] King-Jet Tseng, Yaoming Wang D., Mahinda Vilathgamuwa: An experimentally verified hybrid Cassie-Mayr electric arc model for power electronics simulations, IEEE Transactions on Power Electronics, 12 (1997), no.3, 429-436
<https://ieeexplore.ieee.org/document/575670>
- [11] Sawicki A.: Racjonalizacja modeli hybrydowych łuku elektrycznego. Przegląd Elektrotechniczny (Electrical Review) 2017, R. 93, no. 11, pp. 198-203. (doi:10.15199/48.2017.11.41)
<http://sigma-not.pl/publikacja-110416-2017-11.html>
- [12] Diatczyk J., Jaroszyński L., Komarzyniec G., Stryczewska H. D.: Modelowanie reaktorów ze ślizgającym się wyładowaniem łukowym. Technologie nadprzewodnikowe i plazmowe w energetyce, Chapter 7, p. 207-239. Wyd. Lubelskie Towarzystwo Naukowe, Lublin 2009.
- [13] Janowski T., Jaroszyński L., Stryczewska H. D.: Modification of the Mayr's electric arc model for gliding Arc Analysis. XXVI International Conference on Phenomena in Ionized Gases, Nagoya, Japan 2001/7/17, pp. 341-342
- [14] Верещаго Е.Н., Костюченко В. И.: Модель электрической дуги в MATLAB/Simulink. Электротехника та електроенергетика, 2, 2013. pp. 40-46.
- [15] Marciniak L.: Model of the arc earth-fault for medium voltage networks. Central European Journal of Engineering 2011, No 2, pp. 168-173.
- [16] Sawicki A.: Wykorzystanie charakterystyk statycznych o określonym napięciu zapłonu do modelowania łuków w szerokim zakresie zmian wymuszenia prądowego. Biuletyn Instytutu Spawalnictwa 2019, no. 1, pp. 29-33. (Static characteristics of defined ignition voltage used in the modelling of arc within a wide range of current excitation. pp. 45-52 doi: 10.17729/ebis.2019.1/5)
<http://bulletin.is.gliwice.pl/article/ebis.2019.1/5>
- [17] Sawicki A.: Funkcje wagowe w modelach hybrydowych łuku elektrycznego. Śląskie Wiadomości Elektryczne 2012, no. 5, pp. 15-19.